Theoretical studies of ion bombardment: Many-body interactions

Davy Y. Lo, Tom A. Tombrello, and Mark H. Shapiro
Division of Physics, Mathematics, and Astronomy, California Institute of Technology, Pasadena, California 91125

Barbara J. Garrison and Nicholas Winograd
Pennsylvania State University, University Park, Pennsylvania 16802

Don E. Harrison, Jr.
Department of Physics, U.S. Naval Postgraduate School, Monterey, California 93940

Many-body forces obtained by the embedded-atom method are incorporated into the description of low-energy collisions and surface ejection processes in molecular dynamics simulations of sputtering from metal targets. Bombardment of small, single-crystal Cu targets (400–500 atoms) in three different orientations ({100}, {110}, {111}) by 5-keV Ar^+ ions have been simulated. The results are compared to simulations using purely pairwise additive interactions. Significant differences in the spectra of ejected atoms are found.

I. INTRODUCTION

Computer simulations of sputtering generally have used pair potentials to describe the forces between atoms.[1] Pair potential models assume that the total potential energy of a system of atoms may be expressed as a sum of two-body terms. The pair potential model has been successful in describing bulk properties such as heat of sublimation, bulk modulus, and thermodynamic equations of state.[2] This is surprising because atoms are not point particles. However plausible this may be in cases where the atomic density is macroscopically uniform, the pair potential approximation is rather dubious for processes that involve extreme local nonuniformity of atomic densities such as vacancy formation, surface diffusion, and atomic ejection during sputtering. Pair potential approximations are qualitative at best in other processes that involve surfaces such as fracture, surface segregation, and surface reconstruction. Attempts have been made to include electronic effects by introducing a density-dependent term to the total energy.[3,4] Since the atomic density is only unambiguously defined as an averaged quantity, this method still does not properly account for local density variations.

A simple example will illustrate the many-body forces in atomic interactions. The forces between two isolated atoms consist of the mutual repulsion of the ion cores and the attractive force of the chemical bond which depends directly on the electron distribution. Introduction of a third atom will disturb the original electron distribution and thereby change the force between the first two atoms. The extent of this many-body effect will therefore depend on the polarizability of the atoms. In particular, it will be important in metals. We can always write the total energy as a sum of pair potentials but it will not consistently describe the forces in particular atomic configurations.

This is seen when we compare a pair potential fitted to experimental bulk Cu data with a dimer potential fitted to experimental diatomic data. The bulk Cu potential has a well depth of 0.34 eV (Ref. 2) while the potential energy of a Cu dimer in vacuum has a minimum of 2.03 eV (Ref. 5). The two pair potentials are drastically different. In the case of sputtering from metals the ejection process at the surface will involve dynamical multimer atomic configurations where the many-body effect should play an important role.

To include these many-body effects, we will use the embedded-atom method (EAM) of Daw and Baskes[6] to describe atomic interactions in a molecular dynamics simulation of sputtering. Recent molecular dynamics simulation of sputtering from the (111) face of Rh single crystal employing EAM interactions compared favorably to experimental data.[7] We have simulated the sputtering of Cu single crystals by 5-keV Ar^+ ions in the three low-index orientations ({111}, {110}, {100}) using many-body interactions. The resulting spectra of sputtered atoms will be compared to simulations using purely two-body interactions.

II. INTERACTION POTENTIALS

In the EAM framework, the total potential energy of a system of atoms is, in addition to the usual pairwise sum of pair interactions, a sum over each atomic site i of an embedding function that is a function only of the unperturbed electron density at each site:

$$E=\sum_i\left[F_i\left(\sum_{j\neq i}\rho_{ij}\right)+\frac{1}{2}\sum_{j\neq i}\phi_{ij}\right]. \tag{1}$$

Here E is the total potential energy, F is the embedding function, ϕ is a purely repulsive pair interaction, and ρ is the free-atom electron density (Fig. 1). Furthermore the embedding function depends only on the atomic species in question. This description includes many-body effects which are not well understood in sputtering processes. Since the electron density at each atomic site may be unambiguously defined and the resulting force expressed for each atom is as simple as in the pair potential model, it is possible to incorporate EAM into our molecular dynamics sputtering code without a formidable increase in computation time.

For applications where relatively low energies ($\sim$eV) are involved, $F(\rho)$ and $\phi(r)$ may be obtained from equilibrium experimental data such as sublimation energy, elastic con-

 0734-2101/88/030708-04$01.00

tential used in this paper is different from the one used in a previous molecular dynamics simulation of sputtering from Cu.[11] The pair potential used here has a larger core and its Morse parameters are obtained by fitting to a universal equation of state rather than by the traditional method.[2]

III. SIMULATION RESULTS

The sputtering yields of the EAM calculations are generally lower than that of the pair potential by a factor of 0.71 even though the surface binding energy (SBE) at the surface hole sites are slightly lower in the EAM case (Table I). Here SBE is defined as the energy required to move an atom for an unrelaxed surface hole site to infinity instantaneously. These values of SBE agree reasonably well with the calculations by Jackson.[12] The lack of correlation between the yield and SBE among the different faces is due to their crystalline nature, but this does not explain why EAM gives a lower yield. The relative yields between faces are identical for EAM and pair potential calculations. The ratios of pair potential yield to EAM yield for the three faces are all equal indicating that relative face yields are insensitive to the many-body effect.

The energy distributions of sputtered atoms (integrated over all angles) in the EAM case follow the trend of being dramatically broader while peaking at much higher energies [Figs. 2(a)–2(c)]. Similar results were also obtained by recent molecular dynamics simulations of sputtering from Rh.[7,13] The peak position in the EAM cases is higher by more than a factor of 2 as compared to the pair potential calculations although the SBE's in the two cases are identical. Theoretical[14,15] and experimental[16] studies advocate a peak position at around 0.7 of the experimental heat of sublimation. With an experimental sublimation energy of 3.54 eV for Cu, the pair potential calculation gave a lower peak position than anticipated.

The slow decay of high-energy components in the EAM case would indicate that harder collisions are taking place in the subsurface collision cascade according to Thompson's model of sputtering.[17] However, many-body effects above the surface may play a more important role in contributing to the broadening. Both the distribution broadening and higher peak positions indicate that the EAM approach affects the ejection process in a way that is more subtle than a simple rescaling of atomic binding.

TABLE I. Top: Total sputtering yields. Bottom: Binding energy at surface hole site (SBE).

Face/yield	Pair	EAM
111	7.66 (2.87)[a]	5.38 (2.76)[a]
110	2.67	1.95
100	3.69 (1.38)	2.59 (1.33)
Face/SBE (eV)	**Pair**	**EAM**
111	4.74	4.17
110	4.15	3.90
100	4.58	4.21

[a] These are normalized to the respective 110 face yields.

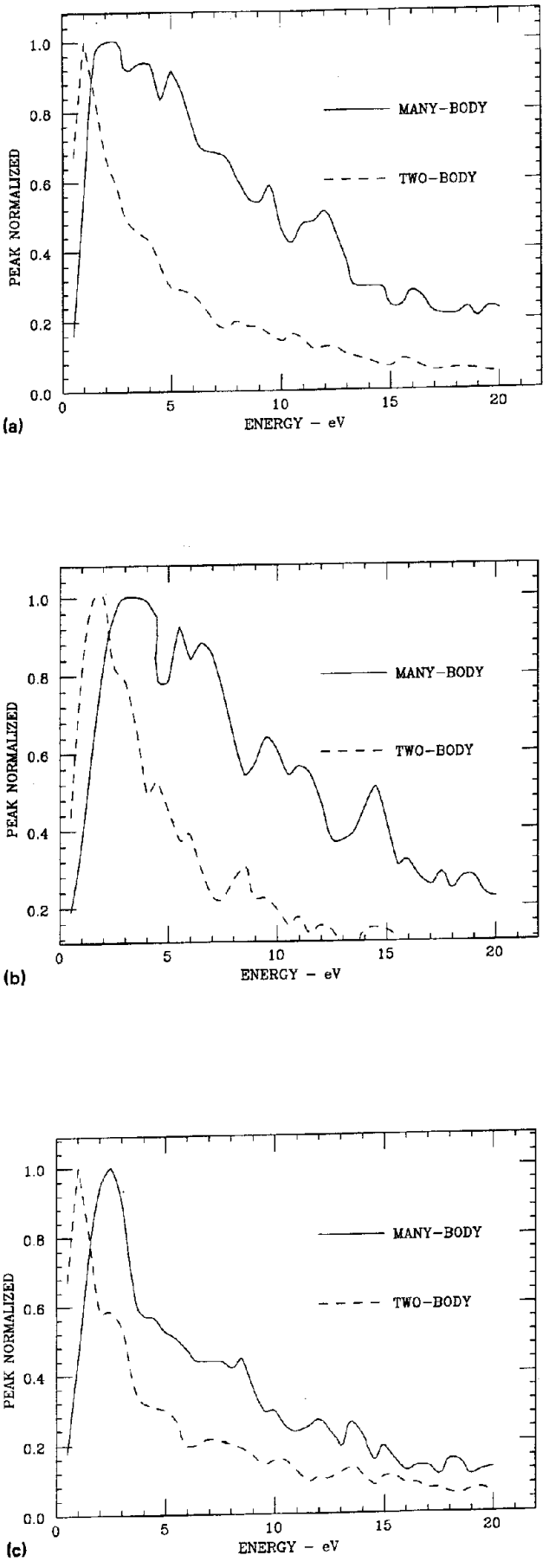

FIG. 2. (a) Energy distribution of sputtered atoms for {111} face, (b) energy distribution of sputtered atoms for {110} face, and (c) energy distribution of sputtered atoms for {100} face.

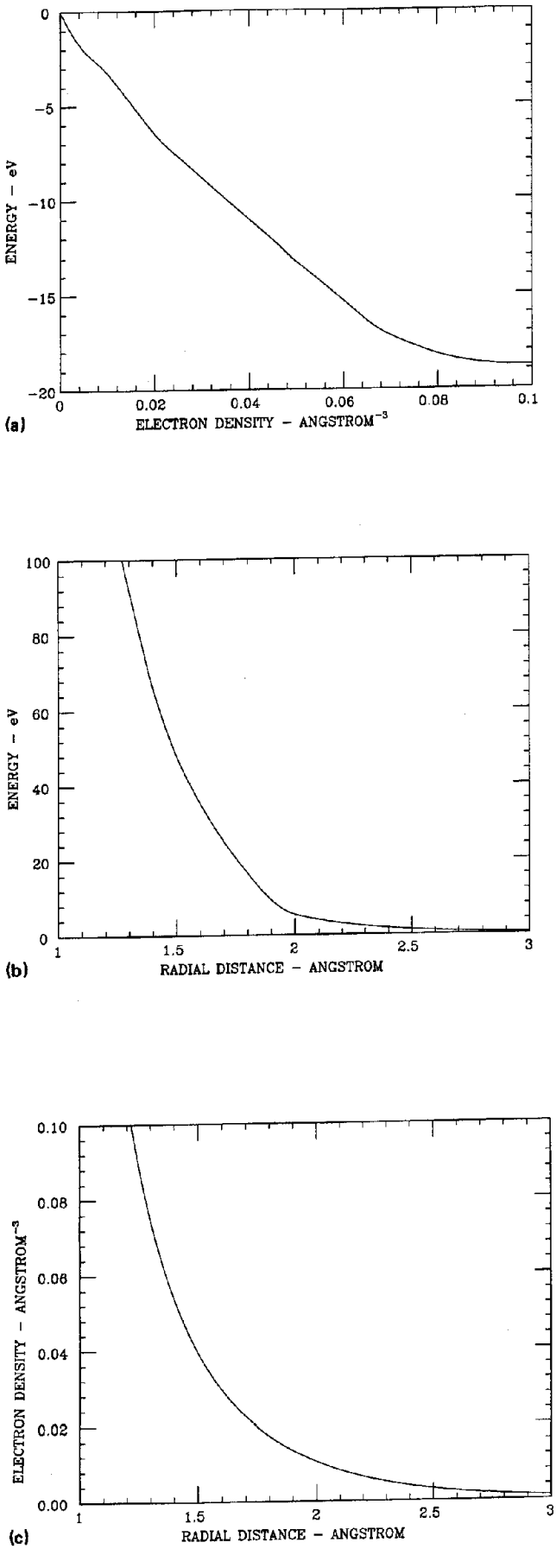

FIG. 1. (a) Embedding function, (b) EAM pair interaction, and (c) free Cu atom electron density.

stants, and vacancy formation energy.[8] However, for processes where higher energies are involved, in particular sputtering, the equilibrium experimental data are hardly adequate since these processes are in general far from equilibrium. For such applications we require the combination F and ϕ to satisfy a semiempirical two-atom interaction $V(r)$ in addition to the experimental equilibrium data. $V(r)$ is related to F and ϕ by

$$V(r) = 2F[\rho(r)] + \phi(r). \tag{2}$$

$V(r)$ is obtained by splining the Moliere function core to an attractive Morse potential. The Moliere screening radius was taken to be the standard Thomas–Fermi screening radius while the Morse parameters were obtained from experimental diatomic ground-state binding energy, vibrational frequency, and equilibrium separation.[5]

Rose *et al.*[9] showed that the energy equation of state U may be written as a universal function of the lattice length scale a. The function U depends on the equilibrium lattice constant, sublimation energy, and bulk modulus parametrically. In terms of $F(\rho)$ and $\phi(r)$ the energy per atom for a crystal is

$$U(a) = F\left(\sum_i \rho(r_i)\right) + \frac{1}{2}\sum_i \phi(r_i). \tag{3}$$

Here the sum is over all neighbors in a lattice of length scale a. $\rho(r)$ was taken from the Hartree–Fock–Slater calculations of Clementi and Roetti.[10] Given ρ, F is uniquely determined by ϕ. By parametrizing $\phi(r)$ (Ref. 8) and writing the elastic constants and vacancy formation energy in terms of F, ϕ, and ρ,[6] we can determine $\phi(r)$ by a least-squares fit with Eq. (3) as a constraint. Once ϕ is determined, F is obtained by varying the lattice length scale about the equilibrium value. So far $F(\rho)$ and $\phi(r)$ have been determined in their respective domains about equilibrium. For large ρ, we let F approach a negative constant (this is rather arbitrary since ϕ will be much larger than F). The linearity of F at large ρ will make the interactions exclusively two body in high-energy collisions. For small ρ, F is given by Eq. (2). The $F(\rho)$ in the two regions are joined smoothly by a spline to obtained the final $F(\rho)$. Now $\phi(r)$ is obtained for all r from Eq. (2). This procedure yields a combination of $F(\rho)$ and $\phi(r)$ that fits to Eq. (2) exactly for all r and to Eq. (3) exactly about the equilibrium while fitting to other experimental equilibrium data in a least-squares sense. Detailed descriptions of the embedded-atom method and fitting of embedded-atom functions to experimental data in the equilibrium region can be found in Refs. 6 and 8.

The exclusively two-body calculation employed a pair potential consisting of the same Moliere core joined by a cubic spline to an attractive Morse function. The Morse function was fitted to the elastic constant C_{11} and the same universal equation of state:

$$U(a) = \frac{1}{2}\sum_i \psi(r_i). \tag{4}$$

Here the sum is over all neighbors of a lattice site as in Eq. (2) and $\psi(r)$ is a Morse function with three parameters. The parameters were adjusted to optimize the fit over a range of length scale variations. It should be noted that the pair po-

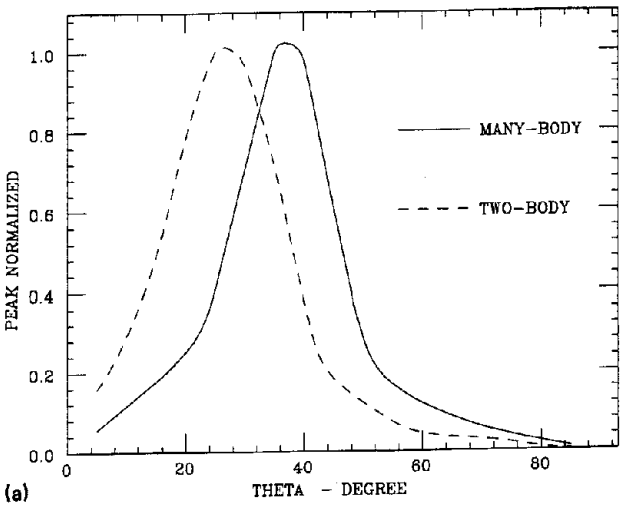

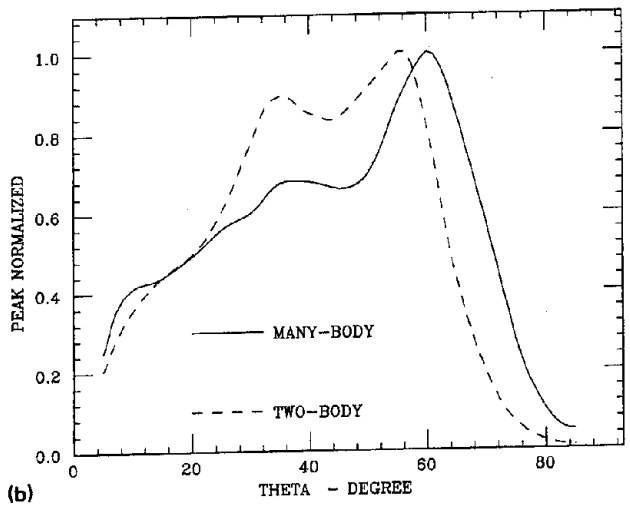

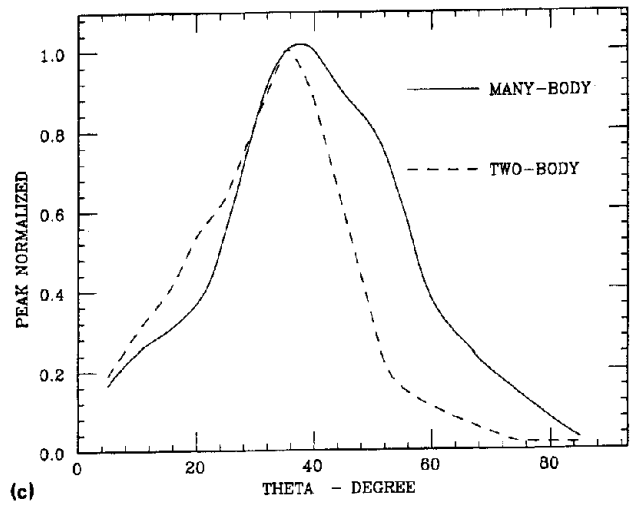

FIG. 3. (a) Polar angular distribution of sputtered atoms for {111} face, (b) polar angular distribution of sputtered atoms for {110} face, and (c) polar angular distribution of sputtered atoms for {100} face.

The differences in the polar angular distribution (integrated over all energies) of sputtered atoms between the two interactions is most notable for the {111} face and less so for the other two faces [Figs. 3(a)–3(c)]. The angular distribution peak position is 12° higher and has a much smaller central spot in the EAM case for the {111} face. The fact that large differences occurred only for the {111} face suggest a changing EAM atomic core size with atomic configuration and a smaller EAM atomic core in surface close-packed configurations.

IV. CONCLUSION

Both the angular and energy spectra calculated with EAM for Cu follow the general trend of recent experimental data[16] and an EAM molecular dynamics simulation[7] for Rh. No attempts such as parametrizing the Thomas–Fermi screening radius have been made to reproduce experimental Cu sputtering data. The important result is that experimental bulk metal data alone are not sufficient to determine interaction potentials for sputtering simulations. Two different rational approaches to describing the dynamics of sputtering capable of reproducing experimental bulk metal properties gave very different spectra of sputtered atoms. Conversely, the detailed data on the energy and angular distributions of sputtered atoms (such as Ref. 16) may contain a great deal of information on atomic interactions at the surfaces of solids and liquids. This is contrary to the commonly held view that a simple effective surface binding energy suffices in describing sputtering phenomena.[18] We make no claim that the EAM approach is the best choice for a comprehensive theory; however, its predictions are distinctively different than those from pair potentials, which indicates that sputtering predictions are sensitive to details of the atomic interaction used.

ACKNOWLEDGMENT

This work was supported in part by the National Science Foundation, Grant No. DMR84-21119.

[1]D. E. Harrison, Jr., Radiat. Eff. **70**, 1 (1983).
[2]L. A. Girifalco and V. G. Weizer, Phys. Rev. **114**, 687 (1959).
[3]R. A. Johnson, Phys. Rev. B **6**, 2094 (1972).
[4]M. I. Baskes and C. F. Melius, Phys. Rev. B **20**, 3197 (1979).
[5]K. P. Huber and G. Herzberg, *Molecular Spectra and Molecular Structure* (Van Nostrand Reinhold, New York, 1979).
[6]M. S. Daw and M. I. Baskes, Phys. Rev. B **29**, 6443 (1984).
[7]B. J. Garrison, N. Winograd, D. M. Deaven, C. T. Reimann, D. Y. Lo, T. A. Tombrello, D. E. Harrison, Jr., and M. H. Shapiro, Phys. Rev. B (submitted).
[8]S. M. Foiles, M. I. Baskes, and M. S. Daw, Phys. Rev. B **33**, 7983 (1986).
[9]J. H. Rose, J. R. Smith, F. Guinea, and J. Ferrante, Phys. Rev. B **29**, 2963 (1984).
[10]E. Clementi and C. Roetti, *Atomic Data and Nuclear Data Tables* (Academic, New York, 1974).
[11]M. H. Shapiro, P. K. Haff, T. A. Tombrello, D. E. Harrison, Jr., and R. P. Webb, Radiat. Eff. **89**, 234 (1985).
[12]D. P. Jackson, Radiat. Eff. **18**, 185 (1973).
[13]B. J. Garrison, N. Winograd, C. T. Reimann, and D. E. Harrison, Jr., Phys. Rev. B **36**, 3516 (1987).
[14]B. J. Garrison, N, Winograd, D. Y. Lo, T. A. Tombrello, M. H. Shapiro, and D. E. Harrison, Jr., Surf. Sci. **180**, L129 (1987).
[15]R. Kelly, Nucl. Instrum. Methods B **18**, 388 (1987).
[16]J. P. Baxter, G. A. Schick, J. Singh, P. H. Kobrin, and N. Winograd, J. Vac. Sci. Technol. A **4**, 1218 (1986).
[17]M. W. Thompson, Philos. Mag. **19**, 377 (1968).
[18]P. Sigmund, Phys. Rev. **184**, 383 (1969).